ARTICLES
PUBLISHED ONLINE: 4 AUGUST 2013 | DOI: 10.1038/NMAT3722
nature materials

A general relationship between disorder, aggregation and charge transport in conjugated polymers

Rodrigo Noriega[1†‡], Jonathan Rivnay[2†‡], Koen Vandewal[2], Felix P. V. Koch[3], Natalie Stingelin[3,4], Paul Smith[3], Michael F. Toney[5] and Alberto Salleo[2*]

Conjugated polymer chains have many degrees of conformational freedom and interact weakly with each other, resulting in complex microstructures in the solid state. Understanding charge transport in such systems, which have amorphous and ordered phases exhibiting varying degrees of order, has proved difficult owing to the contribution of electronic processes at various length scales. The growing technological appeal of these semiconductors makes such fundamental knowledge extremely important for materials and process design. We propose a unified model of how charge carriers travel in conjugated polymer films. We show that in high-molecular-weight semiconducting polymers the limiting charge transport step is trapping caused by lattice disorder, and that short-range intermolecular aggregation is sufficient for efficient long-range charge transport. This generalization explains the seemingly contradicting high performance of recently reported, poorly ordered polymers and suggests molecular design strategies to further improve the performance of future generations of organic electronic materials.

Systematic progress in materials engineering is best guided by a fundamental understanding of the impact of structure—from atomic to microstructural and mesoscopic scales—on functional properties. Structural control at the appropriate length scales combined with knowledge of basic physical processes have given rise to engineering breakthroughs and rational design of new materials. For instance, the understanding of how chain alignment and degree of crystallinity control the mechanical properties of polymers led to the development of fibres with specific strengths exceeding that of steel. Recently, the potential to combine low-cost manufacturing and mechanical robustness while simultaneously engineering optoelectronic properties has spurred great interest in semiconducting polymers[1]. Consequently, devices based on organic semiconductors have reached significant milestones, such as ~10% solar power conversion efficiencies[2] and electron and hole mobilities exceeding 1 $cm^2\ V^{-1}\ s^{-1}$ (refs 3,4). In contrast with other semiconductors, there is no commonly accepted, widely applicable model of charge transport in semiconducting polymers. Depending on the materials, models used to describe charge transport in organic semiconductors include band transport, hopping or multiple trapping and release[1]. Except for dynamic localization[5], most of these models have been adapted from the study of inorganic semiconductors, where atoms are strongly localized on their equilibrium lattice sites. In contrast, conjugated polymers are weakly bonded macromolecules with numerous degrees of conformational freedom, resulting in microstructures varying from completely amorphous to crystalline. Typical crystalline packing in semicrystalline conjugated polymers involves ordered lamellae composed of co-facially stacked molecules that exhibit strong π-orbital overlap (Supplementary Fig. S1).

Based on the observation that inorganic polycrystalline semiconductors often transport charge better than their amorphous analogues, much of the progress in the design of semiconducting polymers was made by pursuing polycrystalline-like microstructures. However, recent polymers based on increasingly complex monomers[3,6–13] seem to refute old paradigms exploited to attain high mobility, such as those involving regioregularity, texture, or crystallinity[10,14–16]. More significantly, highly disordered or even seemingly amorphous polymers now perform as well as semicrystalline materials[4,10].

The interplay between microstructure and electrical properties in conjugated polymers is far from being clearly articulated. This difficulty originates from these materials' intermediate location on the order–disorder scale. Materials that are between (poly)crystalline and amorphous are, in general, poorly understood. In this manuscript, we place in a common context both new data and literature data by applying characterization principles that allow a ranking of conjugated polymers according to their degree of structural disorder. All materials for which there exist relevant data, when processed into their highest-performing microstructure, exhibit a large amount of lattice disorder irrespective of their chemistry or overall degree of crystallinity. Structural disorder is linked to electronic localization within molecular stacks and gives rise to electronic traps, which limit charge transport in high-mobility conjugated polymers. This powerful simplification reveals a general structure–property

[1]Department of Applied Physics, Stanford University, Stanford, California 94305, USA, [2]Department of Materials Science and Engineering, Stanford, California 94305, USA, [3]Department of Materials, ETH Zurich, Zurich 8093, Switzerland, [4]Department of Materials and Centre of Plastic Electronics, Imperial College London, London SW7 2AZ, UK, [5]Stanford Synchrotron Radiation Lightsource (SSRL), SLAC National Accelerator Laboratory, Menlo Park, California 94025, USA. †These authors contributed equally to this work. ‡Present addresses: Department of Chemistry, University of California Berkeley, 94720, USA (R.N.); Department of Bioelectronics, Ecole Nationale Supérieure des Mines, CMP-EMSE, MOC, 13541 Gardanne, France (J.R.).
*e-mail: asalleo@stanford.edu

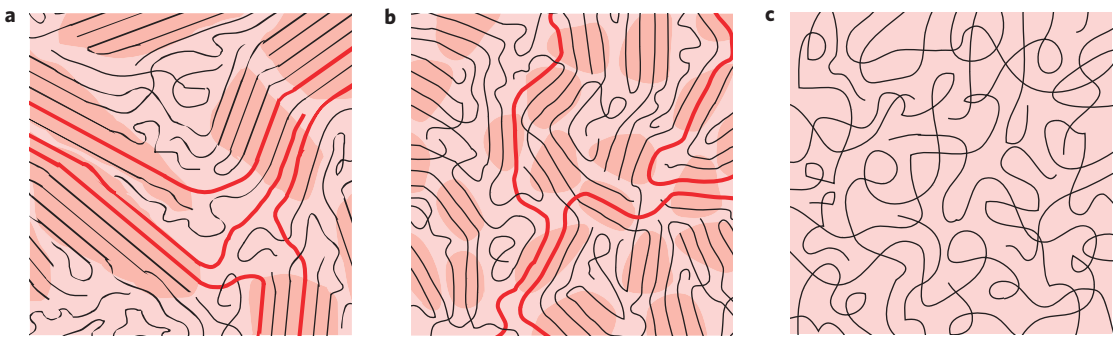

Figure 1 | Microstructure of conjugated polymer films. a–c, Schematics of the microstructure of a semicrystalline polymer film, for example P3HT (**a**), disordered aggregates (**b**) and a completely amorphous film (**c**). Note the coexistence of ordered (darker shadowed areas) and spaghetti-like amorphous regions. This microstructure is similar to the concept of fringed micelles. If the molecular weight is high enough and there is a large enough density of ordered material, long polymer chains (highlighted in red) can connect ordered regions without a significant loss of conjugation, greatly improving charge transport.

relationship relating order at the segmental level to transport at the device scale. A survey of over ten years of literature data confirms the generality of these concepts.

Charge transport and the importance of aggregates

The microstructure of high-molecular-weight poly(3-hexylthiophene), P3HT—a model semicrystalline conjugated polymer—exhibits a continuous variation in order parameters[17,18] where semi-ordered and amorphous 'spaghetti-like' regions coexist; long polymer chains are responsible for the connectivity between adjacent crystallites (Fig. 1a)[19]. Semi-ordered regions may be comprised of large domains with three-dimensional long-range periodicity (crystallites) or smaller domains with short-range ordering of a few molecular units (aggregates, which may also be identified as fringed micelles; Fig. 1b).

In such a heterogeneous microstructure, the ordered regions are largely responsible for charge transport because charges must overcome an energy barrier to move from ordered to amorphous regions. Indeed, owing to its reduced conjugation length, the amorphous fraction of regio-regular P3HT (RR-P3HT) has a larger bandgap compared to the aggregates and we find no evidence of energetic overlap of electronic states in amorphous and ordered P3HT regions (Supplementary Fig. S2). This energetic offset hinders carrier migration into the amorphous regions, and makes it energetically and statistically favourable for charges at the order/disorder interface to migrate back into the ordered regions. Because, in principle, this offset could be reduced by polaronic effects, we test our hypothesis by studying blends of regio-random P3HT (RRa-P3HT) with controlled amounts of RR-P3HT nanofibrils (see Methods)[20]. Even for a low concentration of aggregates (~10% by volume), at current densities comparable to those encountered in electronic devices, the electroluminescence spectra resemble that of RR-P3HT (Fig. 2, and Supplementary Figs S3 and S4). Consequently, transported charges recombine within fibrils. Thus, at realistic current densities, charge carriers remain confined in the ordered regions of a heterogeneous microstructure when such ordered regions are spatially close enough to form an interconnected network through tie-molecules.

This conclusion may be challenged by the oft-encountered assumption, based on calorimetric measurements, that semicrystalline polymer films have a low degree of crystallinity. However, these measurements systematically underestimate the amount of ordered material (Supplementary Fig. S5). In P3HT, we assess that such an underestimation is approximately a factor of two, with the aggregate volume fraction in P3HT films near ~40–50% (refs 21,22). Hence, in high-mobility polymers the fraction of the film comprised of ordered material is sufficiently large to be interconnected by bridging polymer chains, creating a network that sustains efficient charge transport. Such networks of crystallites have been previously observed in conjugated polymers[21,23].

The nature of the connections between aggregates is poorly understood and should be the subject of further study. Nevertheless, we are able to make a few qualitative considerations. Polymer chains are semiflexible[24,25]—that is, rigid at length scales comparable to their persistence length and flexible at larger length scales. If the spacing between neighbouring crystallites is only a few persistence lengths, a chain that exits one ordered region and enters

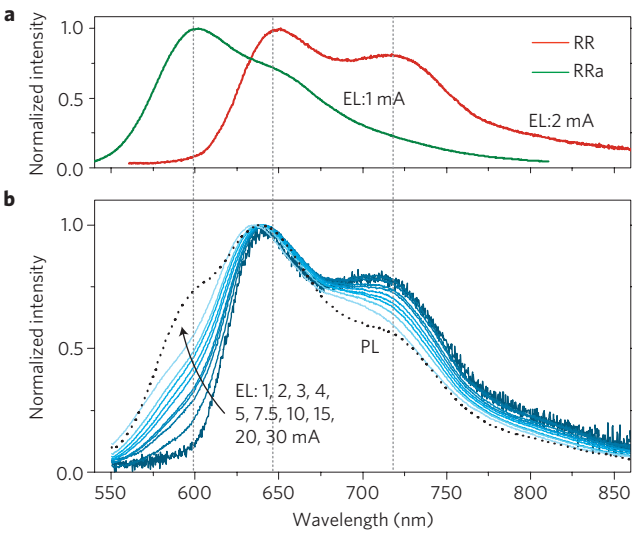

Figure 2 | Photo-physical characterization of pre-aggregated P3HT fibril:amorphous-blend films. a, Reference electroluminescence spectra from pure RR and RRa P3HT. Vertical dashed lines are the electroluminescence peak positions for the amorphous, and 0-0, 0-1 aggregate transitions of the pristine films, respectively. **b**, Photoluminescence spectrum (dotted) showing the signature of aggregated and amorphous material, along with electroluminescence spectra for increasing values of current in the devices made with films of 10% pre-aggregated RR-P3HT. Unlike the photoluminescence spectrum, the low-current (typical of normal device application) electroluminescence spectra show only emission from aggregates, indicating that it is due exclusively to recombination within the aggregates and not to exciton energy transfer to the aggregates before recombination. Only at large current densities does the blue-shifted spectral feature from RRa-P3HT appear, indicating emission from the disordered matrix.

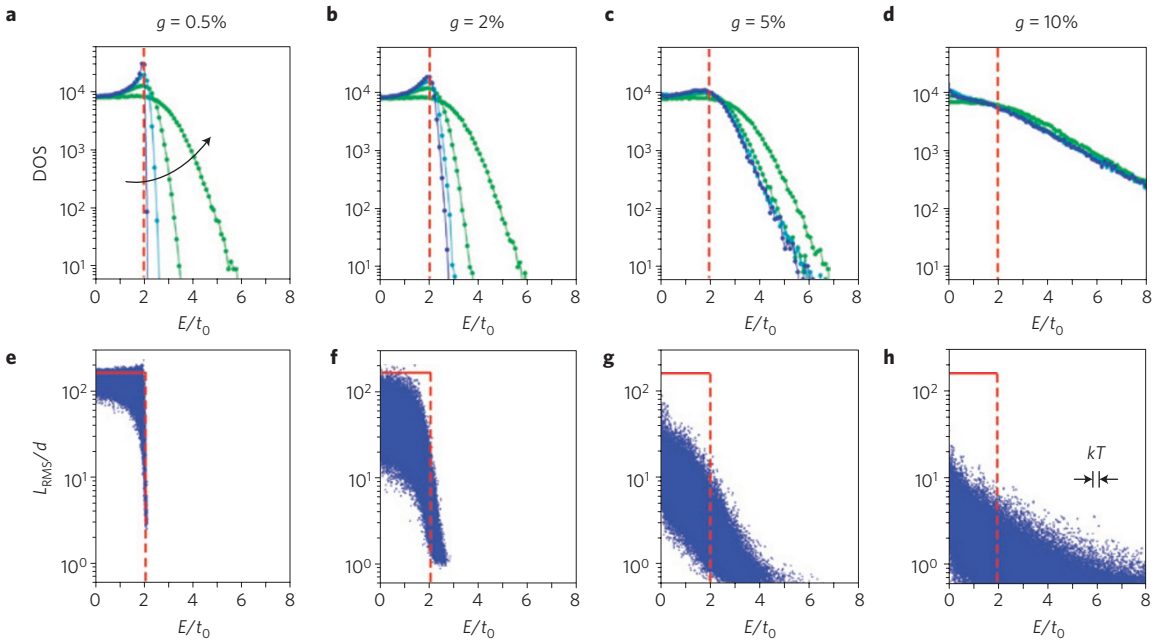

Figure 3 | Modelling of the electronic effects of energetic and structural disorder. a–d, DOS of 1D stacks with different amounts of lattice disorder (g) and Gaussian energetic disorder (of width σ). We show the cases of an almost perfect lattice ($g = 0.5\%$; **a**), a lattice with a small amount of disorder ($g = 2\%$; **b**), a moderately paracrystalline lattice ($g = 5\%$; **c**), and a strongly disordered lattice ($g = 10\%$; **d**). The widths of the probability distribution of on-site energies increase as indicated by the arrow in **a** in the sequence 0, 50, 100 and 200 meV. The energy coordinate is normalized by the inter-site transfer integral at equilibrium, $t_0 = 150$ meV. **e–h**, Localization length (that is, the root mean square spatial extent) for each of the eigenstates of the disordered Hamiltonian, normalized by the inter-site distance d, plotted versus the state's energy. No energetic disorder was included, and the amounts of paracrystalline disorder are the same as **a–d**. The box depicts the localization length of states in a perfect stack (red horizontal line: complete delocalization) and the band edge in the absence of disorder (dashed line). States with a normalized localization length <2 are considered completely localized. The magnitude of kT at room temperature is indicated in **h**.

another should not suffer large bends in its backbone and should retain significant conjugation. Such a chain segment, although not part of any aggregate, provides an efficient charge transport pathway between ordered regions and acts as a tie-molecule (see Supplementary Text). Hence, in high-molecular-weight polymers, transport occurs through an interconnected network of ordered regions. The amorphous fraction of the film does not participate in transport; therefore, the structural properties of the ordered regions govern charge transport in the film. Local mobility measurements in high-molecular-weight P3HT confirm that mobility is limited by transport in these nanoscale aggregates[26], and scanning-probe field-effect measurements show no barrier for charge transport between aggregates[27]. These and our findings demonstrate experimentally that the electrical connection between aggregates is not a rate-limiting step in the transport process for conjugated polymers of sufficiently high molecular weight.

Effect of disorder on the electronic structure of aggregates

As charges in semicrystalline polymers reside in the ordered regions of the film, the effect of structural imperfections in these regions on their electronic properties must be understood. Structural disorder gives rise to energetic disorder—that is, variations in the energy levels across the material—and also affects intermolecular charge transfer integrals. Disorder-induced localization is a well-known occurrence in condensed matter[28,29]. Semiconducting polymers, however, require the understanding of charge transport in intermediate disorder regimes. Structural disorder in an imperfect crystal is described by the paracrystallinity model as random fluctuations in lattice spacings. This disorder is quantitatively measured by the paracrystallinity parameter g, which is the standard deviation of local static lattice fluctuations normalized by the average value of the lattice spacing[30]. Interestingly, paracrystallinity describes the local structure of amorphous silicon more accurately than previously accepted models[31].

The strongest electronic coupling in a polymer is along its backbone, but intermolecular transport is necessary in a typical device as no individual chain can provide macroscopic transport. Disorder in the π-stacks of organic semiconductors is most relevant to transport because this direction supports rate-limiting intermolecular charge transfers. Paracrystallinity in the π-stacks causes the creation of deep tails of electronic states extending into the materials' bandgap with a characteristic energy breadth proportional to g^2 (ref. 32). To compare the effects of structural and energetic disorder on electronic structure, we use a tight-binding model where an aggregate is modelled as a 1D π-stack of molecules (Methods and Supplementary Text). Including variations in the molecular energy levels as well as fluctuations in the intermolecular charge transfer integral yields results useful for qualitative comparisons.

In the case of negligible paracrystallinity, the density of states (DOS) of the 1D π-stack depends on the amount of on-site disorder generating a Gaussian tail of states extending into the bandgap (Fig. 3a). Typical π-stacks of conjugated polymers exhibit moderate amounts of paracrystalline disorder ($g \geq 5\%$; see below). Under these conditions, the DOS of the aggregate is hardly affected by on-site disorder and is determined by the amount of paracrystallinity (Fig. 3c,d).

Our model neglects dynamic effects, which were included in a recent study[33] of charge transport in poly(2,5-bis(3-tetradecylthiophen-2-yl)thieno[3,2,-b]thiophene) (PBTTT), where the authors suggested that dynamic fluctuations and polarization-induced charge stabilization lead to further DOS broadening. Fluctuations of electronic couplings, however, occur on a very fast timescale and must be time-averaged before studying charge transfer events. Although our treatment includes no time

dependence, static cumulative disorder is significant in these materials. Dynamic disorder will induce further fluctuations around the static positions, but these refinements do not qualitatively alter our conclusions.

The spatial extent of the calculated wavefunctions for the disordered stack (Fig. 3e–h) shows that disorder-induced states that lie deeper into the DOS tail are increasingly localized. Even states within the originally 'delocalized band' become more localized with increasing paracrystallinity. In the limit of large positional disorder ($g \sim 10\%$), the distinction between band and tail disappears: a single broad distribution of localized states with a monotonically decreasing DOS extends into the bandgap, reproducing well-known results of electronic structure theory of amorphous materials[34,35]. In the intermediate paracrystallinity regime ($g \sim 3$–7%) we observe a coexistence of localized and delocalized states, indicating that in paracrystalline aggregates charge is transported by a mechanism where mobile charge is temporarily trapped in localized states, akin to multiple trapping and release[1,36].

Measuring paracrystallinity in conjugated polymers

Using X-ray diffraction peak-shape analysis (details in Supplementary Text) we quantify paracrystallinity in polymer crystallites to determine whether this disorder dominates their DOS. In PBTTT, a polymer considered to exhibit an exceptional degree of order[37], we find a highly anisotropic lattice disorder. In the lamellar stacking direction, $g_{lam} = 2.6\%$ owing to side chain interdigitation[38,39]. Long-range lamellar order however does not translate to order in the π-stacks, where $g_{\pi} = 7.3\%$, a value close to that of an amorphous stack. Thus, we conclude that the DOS of a PBTTT π-stack is dictated by paracrystalline disorder.

The low amount of paracrystalline disorder measured in a small molecule film and its small anisotropy (Fig. 4 and Supplementary Table S1) shows that organic solids are not inherently disordered in spite of their weak intermolecular forces. Conversely, the distinguishing feature of polymers is the pronounced disorder in the π-stacking direction. To observe this transition, we use thin films of P3HT with chain lengths of 8 to >2,000 monomers (M_n from 1.33 to >350 kg mol^{-1}), and perform single-peak estimations of the π-stacking disorder (Supplementary Text and Figs S6, S7). When starting from an oligomer and adding monomers to form a high-molecular-weight polymer, paracrystallinity in the π-stacking direction is initially low (comparable to that in polycrystalline films of small molecules) and rises until the incremental effect of adding monomers vanishes and paracrystallinity becomes independent of molecule length (Fig. 4a).

Although P3HT represents a model system, we also explored paracrystallinity in the π-stacking direction of other high-mobility polymers. We collect π-stacking data from over 30 literature cases (Fig. 4a), where conjugated polymers were processed with common solvents and casting techniques. It is apparent that high-molecular-weight semicrystalline polymer semiconductors exhibit a surprisingly common level of minimum lattice disorder ($g \sim 6$–8%). In the direction where intermolecular charge transfer occurs, all high-mobility high-molecular-weight polymers are closer to being amorphous ($g \sim 10$–20%) than crystalline ($g < 1\%$), irrespective of the degree of order in the lamellar stacking direction. The universal dependence of paracrystalline disorder on molecular weight indicates that chain folding and entanglements are probable sources of defects[40]. Side-chain conformational disorder may also disrupt the backbone packing arrangement, leading to an intrinsic level of disorder common to all conjugated polymers.

A simultaneous comparison of the effect of molecular weight on disorder and on mobility (Fig. 4) is a strong indication that charge transport is linked to lattice disorder. When the molecular weight of P3HT is high enough such that its lattice disorder becomes independent of chain length, the carrier mobility is also

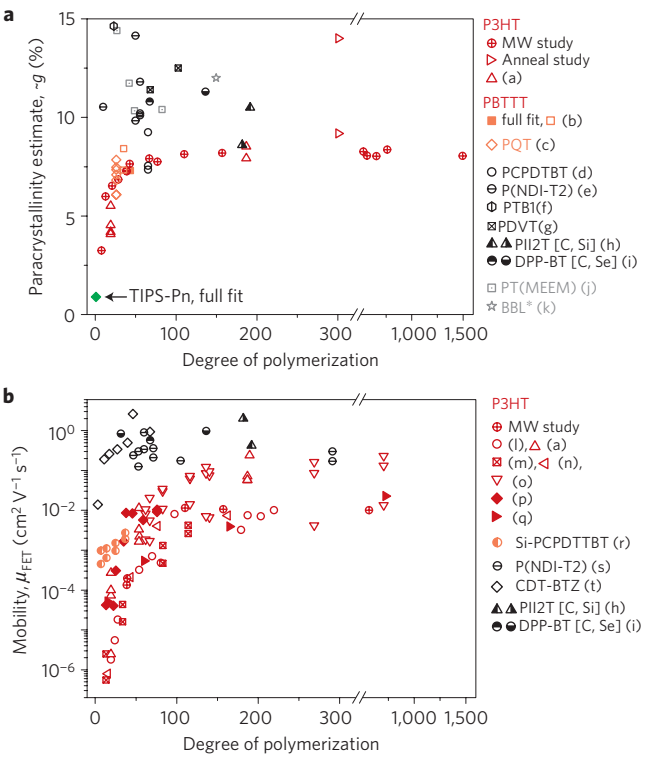

Figure 4 | Chain length effects on paracrystallinity and charge transport. **a**, The π-stacking paracrystallinity in films of polymeric semiconductors of different molecular weight (MW), plotted as a function of degree of polymerization. Semicrystalline materials (P3HT, PBTTT, PQT) are shown in shades of red. Poorly ordered high performing materials are shown in black. Others are shown in grey. Open symbols are estimates, solid symbols are derived from a full analysis. As a comparison, cumulative disorder in polycrystalline triisopropylsilyl pentacene (TIPS-Pn) is far smaller than that of PBTTT and, importantly, shows significantly less anisotropy (Supplementary Table S1). **b**, Mobility as a function of molecular weight for a variety of semiconducting polymers. P3HT is shown in red with different symbols referring to different studies. Other high-performing materials are shown in black. For the complete list of references see Supplementary Text.

remarkably independent of chain length. The link between these two fundamentally different properties is particularly striking, as the turn-over point is the same for both (chains with 50–100 monomers for P3HT) and agrees with recent yield and mobility measurements of photogenerated charges[41]. Our findings remain valid, irrespective of whether interface or bulk measurements are considered (see Supplementary Text). Similar improvements in mobility with increasing molecular weight have been observed in other polymers[11,42].

The effect of molecular weight on charge transport in semicrystalline polymers is subject to an intrinsic and general trade-off. Long chains provide electrical connectivity between ordered regions, allowing efficient charge transport, but also result in higher structural disorder. In the low-molecular-weight connectivity-limited regime, mobility rises quickly as average chain length increases[43]. Eventually, the mobility plateaus as a function of molecular weight when enough connectivity is provided for charge to move through the paracrystalline regions (see Supplementary Text). Thus, in high-molecular-weight polymers charge transport is strongly enhanced by the connectivity of the ordered regions (crystallites and aggregates) but limited by lattice disorder in these regions once sufficient connectivity is established.

The spread in mobility values is significant, showing that no single microstructural feature is entirely responsible for electronic

performance. Differences in morphology arise from variations in processing conditions and polydispersity, which contribute to the variability in charge carrier mobility. Despite these factors, the fundamental transport-limiting mechanism and its causal connection to paracrystallinity is preserved.

Paracrystallinity governs charge transport

In 'classic' (that is, designed to exhibit a noticeable degree of crystallinity and extended π–π stacking) semicrystalline conjugated polymers, paracrystalline disorder in the crystallites limits charge transport via the introduction of traps. The level of lattice disorder in the π-stacking direction measured in all high-molecular-weight polymers corresponds to the regime where localized and delocalized states in the aggregates coexist, giving rise to trapping-limited transport, as experimentally observed in field effect transistors (FET) and in local mobility measurements[26]. In FETs, the difference in energy between the populated traps and the mobile states manifests itself in the activation energy for transport and its dependence on charge density (gate voltage). Hence, the greater the disorder, the deeper the traps and the larger the activation energy.

In Fig. 5, we gather activation energies derived from temperature-dependent FET measurements, and trap depth/tail widths derived from modelling electrical transport both from the literature and from this work. These data were collected from samples spanning a range of mobility, materials purity, device preparation, surface treatments and geometry. In spite of such variety of materials and conditions, a consistent behaviour emerges. Transport in common thiophene-based semicrystalline polymers—for example, P3HT, poly[5,5′-bis(3-alkyl-2-thienyl)-2,2′-bithiophene] (PQT), PBTTT—has an average 72 ± 24 meV activation energy. In comparison, completely amorphous materials show a significantly higher average activation energy $\sim 230 \pm 100$ meV. It is interesting to examine new high-performance polymers, which do not seem to belong in either category. Examples of these materials are copolymers based on more complex moieties, such as naphthalene-diimides (PNDI-T2), diketopyrrolopyrroles with sulphur and selenium (DPP-BT, DSePP-BT), and carbazoles (PCDTBT), but also newer materials such as isoindigo copolymers and indacenodithiophene-based polymers. These materials have mobilities comparable to those of semicrystalline polymers ($\mu_{FET} \sim 1\ cm^2\ V^{-1}\ s^{-1}$), but at first glance, morphologically, they are closer to the amorphous materials family. Indeed their disorder is higher than that of semicrystalline polymers, as evidenced by lower diffracted intensities, fewer observable diffraction peaks, and/or the large breadth of their π-stacking peak. These new high-mobility polymers exhibit activation energies and trap breadths of 76 ± 33 meV: similar to those of 'classic' semicrystalline polymers and significantly lower than the mean value observed for amorphous conjugated polymers. Many of these new reportedly 'amorphous' materials have at least enough short-range order to result in detectable diffraction in synchrotron XRD experiments (Supplementary Fig. S8). Though polymers in this new class are seemingly disordered, they exhibit the tell-tale signs of aggregation in their solid-state optical absorption spectra, namely the presence of a resolvable vibronic progression near the absorption edge[22]. Short-range order in the form of aggregates is sufficient to support efficient intermolecular charge transfer. Because charges have a short scattering mean free path in the π-stacks—on the order of a nanometre[36]—they are mostly affected by such short-range order. Disordered crystallites larger than a scattering length bring hardly any additional benefit for charge transport. In conjugated polymers, crystallinity—no matter how low—is a sign that the polymer chains have a tendency to form stacked aggregates with a paracrystallinity that can be estimated by the width of the π-stacking XRD peak. This collection of interconnected aggregates enables high mobilities in high-molecular-weight polymers despite the consistently large

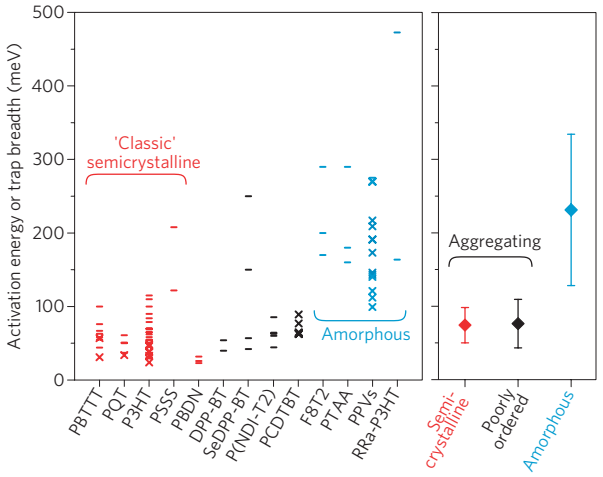

Figure 5 | Activation energy for transport in semiconducting polymers. Activation energies obtained from FET data from this work, and from the literature (dash), as well as trap depth/tail widths derived from device modelling (cross) for traditional classic semicrystalline materials (red), new high performers that are found to be poorly ordered (black), and completely amorphous materials (blue). Data (84 values for 13 different materials) are binned by material (for the complete list of references see Supplementary Text). The averages and standard deviations from the respective groups are shown for semicrystalline, poorly ordered, and amorphous materials on the right panel.

paracrystalline disorder in the π-stacking direction and weak diffracted intensities.

Molecular stacking, even with only short-range order, makes aggregating materials fundamentally different from truly amorphous polymers. Assuming an exponential dependence of the intermolecular transfer integral t on separation x, $t = t_0 e^{-\beta x}$, the prefactor t_0 and wavefunction overlap decay length $(1/\beta)$ govern the extent to which lattice disorder affects charge transport. The newer high-mobility polymers can tolerate nanometre-scale disorder owing to their structure at the ångström-scale. For example, increasing t_0 by reducing the π–π stacking distance causes aggregates to be electronically less sensitive to large amounts of disorder, increasing the threshold beyond which paracrystallinity-induced states severely affect transport. Similarly, reducing β by designing materials with orbitals having larger overlaps or favourable symmetries reduces the effect of positional disorder on charge transport. Some of these factors are probably at work in recently reported high-mobility polymers. The optimization of side-chains to increase solubility leads to a reduced intermolecular π-stacking distance in diketopyrrolopyrrole-furan and isoindigo-based polymers. Using large and planar fused-ring aromatic cores increases the overlapping area between adjacent π-stacked units, making the aggregates less sensitive to positional disorder[12,13]. Therefore, tuning the molecular design to improve packing and orbital shape, orientation and symmetry may contribute to making transport in aggregates—where charge is confined—less sensitive to π-stacking disorder, thereby preserving efficient device-scale charge transport.

These considerations separate polymeric semiconductors into two classes. In one class we have truly amorphous materials, lacking any long-range order and characterized by broad, featureless amorphous X-ray scattering halos. Charge transport in these truly amorphous materials is limited by hopping between localized states in a broad DOS. Such a transport mode is restricted to mobilities $<0.1\ cm^2\ V^{-1}\ s^{-1}$ and is subject to large activation energies[44]. In the second class are materials that can form interconnected aggregates exhibiting at least short-range order, with transport in field-effect devices described by a multiple trapping and release mechanism.

The difference between aggregating materials families is the distance over which aggregation persists: semi-crystalline materials exhibit relatively long range order (several to 10 s of nanometres in the π-stacking direction as derived from the coherence length) and strong X-ray scattering, whereas weakly scattering polymers can be ordered in some crystallographic directions (alkyl-stacking) but remain largely disordered in the π-stacking direction (Supplementary Fig. S8). Even though these semi-amorphous materials are strongly disordered in their π-stacks, their ability to form aggregates allows locally efficient intermolecular charge transport. Such short-range order at the segmental level is sufficiently pervasive in the thin-film microstructures to provide effective pathways for charge transport. Aggregating polymers of high molecular weight, whether very weakly diffracting or truly semicrystalline, belong to the same class, where the disorder in the intermolecular π-stacking direction is consistently high in all conjugated polymers and induces traps in the DOS, which are transport-limiting.

Implications for high-mobility semiconducting polymers

Understanding charge transport in conjugated semicrystalline polymers has proved to be a challenging problem owing to the unusual range of disorder they exhibit. These materials are not well-ordered, yet they are not amorphous either. By bringing together data from years of research in conjunction with new insights, we formulate a link between the molecular- and micro-structure of high-mobility semiconducting polymers and their macroscopic electrical properties. These insights uncover strong similarities within seemingly diverse families of conjugated polymers and allow us to formulate a unified transport model. We find that, in the π-stacking direction, the lowest observed amount of lattice disorder in all high-performance—and necessarily high molecular weight—polymers is unexpectedly large and remarkably independent of material. The unifying requirement for high carrier mobility is the presence of interconnected aggregates, even if they are small and disordered. The key to designing high-mobility polymers is not in increasing crystallinity but rather in increasing their tolerance to an inevitably large amount of disorder within the aggregates by allowing more efficient intra- and intermolecular charge transport/transfer at the segmental level. The fundamental relationship presented here between short-range order in π-aggregates, aggregate connectivity, and macroscopic charge transport provides input for the design of new optoelectronic polymers with the potential to usher in technological successes comparable to those obtained with high-strength polymers. More broadly, we provide a general framework for understanding how to take advantage of intermediate order at different length scales to control the macroscopic properties of semicrystalline polymers, be they optical, electrical or mechanical.

Methods

Sample preparation. Samples for structural determination and TFT measurements were prepared on native oxide silicon and 200 nm thermal oxide silicon, respectively. Substrates were sonicated in acetone and isopropyl alcohol before drying with nitrogen and undergoing ultraviolet ozone treatment (20 min). Raw materials were used as received from Merck Chemicals (TIPS-Pn, P3HT), Polyera (N2200, and derivatives), Imperial College London (P3HT, PBTTT), and ETH Zurich (P3HT, P3HT-oligomers). Films were spin cast from ~10 mg ml^{-1} solutions at 1,000–1,500; if used for electro-optical testing film formation was performed in a N_2 glove box (<1 ppm O_2). The samples in the P3HT molecular weight series were cast from toluene, whereas other films (TIPS-Pn, P3HT, P[NDI2OD-T2], PBTTT) were cast from dichlorobenzene. Directional samples of PBTTT were cast as previously described[45].

Photo-physical characterization. For electroluminescence (EL) and photoluminescence (PL) studies, we prepared solution blends of RRa-P3HT (M_w = 90 kDa, M_n = 30 kDa) and pre-aggregated RR-P3HT (regio-regularity ~97%, M_w = 105 kDa, M_n = 60 kDa). Starting solutions of RR- and RRa-P3HT in dichlorobenzene (DCB, 30 mg ml^{-1}) were dissolved at 80 °C overnight. To vary the amount of aggregated material in the films, the starting solutions of RR- and RRa-P3HT in DCB were diluted with ethylacetate (2:1 DCB:EtOAc solvent ratio) to form the stock solutions for pre-aggregated and amorphous materials, which were then mixed in 1:1 and 1:9 ratios. Films made from these solutions were spun cast onto ITO/PEDOT substrates and Ca/Al electrodes were evaporated to form devices with an area of 0.1 cm^2. The EL and PL spectra for these devices were collected using a cooled CCD camera and corrected for the spectrometer response. PL experiments used a pump beam from a 535 nm diode laser. The driving voltage for the diodes used in the EL measurements was provided by a Keithley 2400 power source. All these measurements and sample preparation were performed in an inert atmosphere.

Electrical characterization. For devices used for electrical characterization, substrates were first treated with an octadecyltrichlorosilane (OTS) self-assembled monolayer before casting of semiconducting polymer. The top 100 nm Au source and drain contacts were evaporated on dry films. Thin-film transistor devices were characterized in a vacuum probe station evacuated to 10^{-4} mbar. The TFT charge carrier mobility was extracted in the saturation regime ($V_d = -60$ V).

X-ray characterization. X-ray scattering was performed at the Stanford Synchrotron Radiation Lightsource (SSRL) on beamlines 7-2 (high-resolution grazing incidence), 2-1 (high-resolution specular), and 11-3 (2D scattering with an area detector, MAR345 image plate, at grazing incidence). The incident energy was 8 keV for beamlines 7-2 and 2-1, and 12.7 keV for beamline 11-3. The diffracted beam was collimated with 1 milliradian Soller slits for high-resolution in-plane scattering and with two 1 mm slits for specular diffraction. For both grazing incidence experiments, the incidence angle was slightly larger than the critical angle, ensuring that we sampled the full film depth. All X-ray measurements were performed in a helium-filled chamber to minimize beam damage and reduce air scattering. Data are expressed as a function of the scattering vector $q = 4\pi * \sin(\theta)/\lambda$, where θ is half the scattering angle and λ is the wavelength of the incident radiation. Here, q_{xy} (q_z) is the component of the scattering vector parallel (perpendicular) to the substrate. Only high-resolution measurements were employed for extraction of peak parameters and analysis of paracrystalline disorder. Details of the peak shape analysis, and resulting estimates and their justification can be found in the Supplementary Information and in ref. 46.

Simulations. The model from ref. 32 is simplified to a one-dimensional disordered stack made up of N_s sites. A tight-binding Hamiltonian is employed to describe transport through this system, with on-site energies ε_i and nearest neighbour transfer integrals t_i. In the matrix form of the Hamiltonian, the main diagonal reflects the on-site energies and the off-diagonal terms reflect inter-site couplings. To first order, we treat the observed fluctuation in lattice parameter within the crystalline regions only as a distribution of intermolecular separations, neglecting details of molecular orientation and correlations. Energetic disorder was introduced by selecting the on-site energies from a probability distribution of a given width; structural disorder is modelled by varying the coupling between neighbours as $t_i = t_0 e^{-\beta x_i}$, where the bond fluctuations x_i due to lattice disorder modify the transfer integral at equilibrium t_0 with an exponential decay with characteristic length $1/\beta$. The transfer integral was parametrized according to values previously obtained for PBTTT (ref. 32). Solving for the eigenfunctions and eigenvalues of the Hamiltonian yields the states of the system and their energies, respectively.

Received 18 January 2013; accepted 25 June 2013; published online 4 August 2013

References

1. Klauk, H. *Organic Electronics II: More Materials and Applications* (Wiley-VCH, 2012).
2. He, Z. *et al.* Enhanced power-conversion efficiency in polymer solar cells using an inverted device structure. *Nature Photon.* **6,** 593–597 (2012).
3. Chen, H. *et al.* Highly π-extended copolymers with diketopyrrolopyrrole moieties for high-performance field-effect transistors. *Adv. Mater.* **24,** 4618–4622 (2012).
4. Facchetti, A. π-conjugated polymers for organic electronics and photovoltaic cell applications. *Chem. Mater.* **23,** 733–758 (2010).
5. McMahon, D. P. & Troisi, A. Organic semiconductors: Impact of disorder at different timescales. *ChemPhysChem* **11,** 2067–2074 (2010).
6. Chen, Z. *et al.* High-performance ambipolar diketopyrrolopyrrole-thieno[3,2-b]thiophene copolymer field-effect transistors with balanced hole and electron mobilities. *Adv. Mater.* **24,** 647–652 (2012).
7. Jung, J. W., Liu, F., Russell, T. P. & Jo, W. H. A high mobility conjugated polymer based on dithienothiophene and diketopyrrolopyrrole for organic photovoltaics. *Energy Environ. Sci.* **5,** 6857–6861 (2012).
8. Kronemeijer, A. J. *et al.* A selenophene-based low-bandgap donor–acceptor polymer leading to fast ambipolar logic. *Adv. Mater.* **24,** 1558–1565 (2012).

9. McCulloch, I. *et al.* Design of semiconducting indacenodithiophene polymers for high performance transistors and solar cells. *Acc. Chem. Res.* **45,** 714–722 (2012).
10. Zhang, W. *et al.* Indacenodithiophene semiconducting polymers for high-performance, air-stable transistors. *J. Am. Chem. Soc.* **132,** 11437–11439 (2010).
11. Tsao, H. N. *et al.* Ultrahigh mobility in polymer field-effect transistors by design. *J. Am. Chem. Soc.* **133,** 2605–2612 (2012).
12. Mei, J., Kim, D. H., Ayzner, A. L., Toney, M. F. & Bao, Z. Siloxane-terminated solubilizing side chains: Bringing conjugated polymer backbones closer and boosting hole mobilities in thin-film transistors. *J. Am. Chem. Soc.* **133,** 20130–20133 (2011).
13. Yiu, A. T. *et al.* Side-chain tunability of furan-containing low-band-gap polymers provides control of structural order in efficient solar cells. *J. Am. Chem. Soc.* **134,** 2180–2185 (2012).
14. Sirringhaus, H. *et al.* Two-dimensional charge transport in self-organized, high-mobility conjugated polymers. *Nature* **401,** 685–688 (1999).
15. McMahon, D. P. *et al.* Relation between microstructure and charge transport in polymers of different regioregularity. *J. Phys. Chem. C* **115,** 19386–19393 (2011).
16. Rivnay, J. *et al.* Unconventional face-on texture and exceptional in-plane order of a high mobility n-type polymer. *Adv. Mater.* **22,** 4359–4363 (2010).
17. Watts, B., Schuettfort, T. & McNeill, C. R. Mapping of domain orientation and molecular order in polycrystalline semiconducting polymer films with soft x-ray microscopy. *Adv. Funct. Mater.* **21,** 1122–1131 (2011).
18. Collins, B. A. *et al.* Polarized X-ray scattering reveals non-crystalline orientational ordering in organic films. *Nature Mater.* **11,** 536–543 (2012).
19. Grevin, B., Rannou, P., Renaud, P., Pron, A. & Travers, J-P. Scanning tunneling microscopy investigations of self-organized poly(3-hexylthiophene) two-dimensional polycrystals. *Adv. Mater.* **15,** 881–884 (2003).
20. Scharsich, C. *et al.* Control of aggregate formation in poly(3-hexylthiophene) by solvent, molecular weight, and synthetic method. *J. Polym. Sci. B* **50,** 442–453 (2012).
21. Zen, A. *et al.* Effect of molecular weight on the structure and crystallinity of poly(3-hexylthiophene). *Macromolecules* **39,** 2162–2171 (2006).
22. Clark, J., Chang, J-F., Spano, F. C., Friend, R. H. & Silva, C. Determining exciton bandwidth and film microstructure in polythiophene films using linear absorption spectroscopy. *Appl. Phys. Lett.* **94,** 163306 (2009).
23. Takacs, C. J. *et al.* Remarkable order of a high-performance polymer. *Nano Lett.* **13,** 2522–2527 (2013).
24. McCulloch, B. *et al.* Polymer chain shape of poly(3-alkylthiophenes) in solution using small-angle neutron scattering. *Macromolecules* **46,** 1899–1907 (2013).
25. Spakowitz, A. J. & Wang, Z-G. Exact results for a semifexible polymer chain in an aligning field. *Macromolecules* **37,** 5814–5823 (2004).
26. Pingel, P. *et al.* Temperature-resolved local and macroscopic charge carrier transport in thin P3HT layers. *Adv. Funct. Mater.* **20,** 2286–2295 (2010).
27. Bolsée, J-C., Oosterbaan, W. D., Lutsen, L., Vanderzande, D. & Manca, J. The importance of bridging points for charge transport in webs of conjugated polymer nanofibers. *Adv. Funct. Mater.* **23,** 862–869 (2013).
28. Kondov, S. S., McGehee, W. R., Zirbel, J. J. & DeMarco, B. Three-dimensional Anderson localization of ultracold matter. *Science* **334,** 66–68 (2011).
29. Gomez-Navarro, C. *et al.* Tuning the conductance of single-walled carbon nanotubes by ion irradiation in the Anderson localization regime. *Nature Mater.* **4,** 534–539 (2005).
30. Hindeleh, A. M. & Hosemann, R. Paracrystals representing the physical state of matter. *J. Phys. C* **21,** 4155–4170 (1988).
31. Treacy, M. M. J. & Borisenko, K. B. The local structure of amorphous silicon. *Science* **335,** 950–953 (2012).
32. Rivnay, J. *et al.* Structural origin of gap states in semicrystalline polymers and the implications for charge transport. *Phys. Rev. B* **83,** 121306 (2011).
33. Poelking, C. *et al.* Characterization of charge-carrier transport in semicrystalline polymers: Electronic couplings, site energies, and charge-carrier dynamics in poly(bithiophene-alt-thienothiophene) [PBTTT]. *J. Phys. Chem. C* **117,** 1633–1640 (2013).
34. Baldo, M. A., Soos, Z. G. & Forrest, S. R. Local order in amorphous organic molecular films. *Chem. Phys. Lett.* **347,** 297–303 (2001).
35. Pasveer, W. F. *et al.* Unified description of charge-carrier mobilities in disordered semiconducting polymers. *Phys. Rev. Lett.* **94,** 206601 (2005).
36. Street, R. A., Northrup, J. E. & Salleo, A. Transport in polycrystalline polymer thin-film transistors. *Phys. Rev. B* **71,** 165202 (2005).
37. Zhang, X. *et al.* In-plane liquid crystalline texture of high-performance thienothiophene copolymer thin films. *Adv. Funct. Mater.* **20,** 4098–4106 (2010).
38. Kline, R. J. *et al.* Critical role of side-chain attachment density on the order and device performance of polythiophenes. *Macromolecules* **40,** 7960–7965 (2007).
39. Cho, E. *et al.* Three-dimensional packing structure and electronic properties of biaxially oriented poly(2,5-bis(3-alkylthiophene-2-yl)thieno-[3,2-b]thiophene) films. *J. Am. Chem. Soc.* **134,** 6177–6190 (2012).
40. Brinkmann, M. & Rannou, P. Molecular weight dependence of chain packing and semicrystalline structure in oriented films of regioregular poly(3-hexylthiophene) revealed by high-resolution transmission electron microscopy. *Macromolecules* **42,** 1125–1130 (2009).
41. Reid, O. G. *et al.* The influence of solid-state microstructure on the origin and yield of long-lived photogenerated charge in neat semiconducting polymers. *J. Polym. Sci. B* **50,** 27–37 (2012).
42. Tong, M. *et al.* Higher molecular weight leads to improved photoresponsivity, charge transport and interfacial ordering in a narrow bandgap semiconducting polymer. *Adv. Funct. Mater.* **20,** 3959–3965 (2010).
43. Kline, R. J. *et al.* Dependence of regioregular poly(3-hexylthiophene) film morphology and field-effect mobility on molecular weight. *Macromolecules* **38,** 3312–3319 (2005).
44. Troisi, A. The speed limit for sequential charge hopping in molecular materials. *Org. Electron.* **12,** 1988–1991 (2011).
45. DeLongchamp, D. M. *et al.* Controlling the orientation of terraced nanoscale ribbons of a poly(thiophene) semiconductor. *ACS Nano* **3,** 780–787 (2009).
46. Rivnay, J., Noriega, R., Kline, R. J., Salleo, A. & Toney, M. F. Quantitative analysis of lattice disorder and crystallite size in organic semiconductor thin films. *Phys. Rev. B* **84,** 045203 (2011).

Acknowledgements

We thank G. Rumbles for his comments in the preparation of this manuscript. We gratefully thank A. Facchetti and Z. Chen (Polyera, Skokie, IL), and I. McCulloch and M. Heeney (Imperial College, London) for supplying materials (P[NDI2OD-T2], P3HT, and PBTTT). This work is supported by the Center for Advanced Molecular Photovoltaics Award No. KUS-C1-015-21 made by King Abdullah University of Science and Technology (KAUST) (R.N., J.R., K.V., A.S.), and NSF (J.R., A.S.). N.S. acknowledges support by a European Research Council (ERC) Starting Independent Researcher Fellowship under the grant agreement No. 279587. Portions of this research were carried out at the Stanford Synchrotron Radiation Lightsource, a national user facility operated by Stanford University on behalf of the US Department of Energy, Office of Basic Energy Sciences.

Author contributions

A.S., J.R. and R.N. conceived the research. J.R., R.N., K.V. and F.P.V.K. prepared samples for optoelectronic and structural measurements. J.R. and R.N. carried out the XRD experiments and analysed the data. R.N. and K.V. performed the electrical and optical measurements. R.N. performed the simulations. M.F.T., P.S. and N.S. assisted with data interpretation. R.N., J.R. and A.S. wrote the manuscript and all authors participated in manuscript preparation and editing.

Additional information

Supplementary information is available in the online version of the paper. Reprints and permissions information is available online at www.nature.com/reprints. Correspondence and requests for materials should be addressed to A.S.

Competing financial interests

The authors declare no competing financial interests.